Topological Constraints in Directed Polymer Melts

Pablo Serna,[1,2] Guy Bunin,[3] and Adam Nahum[3]
[1]Theoretical Physics, Oxford University, 1 Keble Road, Oxford OX1 3NP, United Kingdom
[2]Departamento de Física—CIOyN, Universidad de Murcia, Murcia 30.071, Spain
[3]Department of Physics, Massachusetts Institute of Technology, Cambridge, Massachusetts 02139, USA
(Received 23 July 2015; published 25 November 2015)

Polymers in a melt may be subject to topological constraints, as in the example of unlinked polymer rings. How to do statistical mechanics in the presence of such constraints remains a fundamental open problem. We study the effect of topological constraints on a melt of directed polymers, using simulations of a simple quasi-2D model. We find that fixing the global topology of the melt to be trivial changes the polymer conformations drastically. Polymers of length L wander in the transverse direction only by a distance of order $(\ln L)^{\zeta}$ with $\zeta \simeq 1.5$. This is strongly suppressed in comparison with the Brownian $L^{1/2}$ scaling which holds in the absence of the topological constraint. It is also much smaller than the predictions of standard heuristic approaches—in particular the $L^{1/4}$ of a mean-field-like "array of obstacles" model—so our results present a sharp challenge to theory. Dynamics are also strongly affected by the constraints, and a tagged monomer in an infinite system performs logarithmically slow subdiffusion in the transverse direction. To cast light on the suppression of the strands' wandering, we analyze the topological complexity of subregions of the melt: the complexity is also logarithmically small, and is related to the wandering by a power law. We comment on insights the results give for 3D melts, directed and nondirected.

DOI: 10.1103/PhysRevLett.115.228303 PACS numbers: 82.35.Lr, 36.20.Ey, 61.25.he, 83.80.Sg

The fact that polymer chains cannot pass through each other is the crucial factor in their dynamics, underlying for example the reptation picture [1–3], and in various situations also determines their equilibrium state. Two salient examples are a single ring polymer and a melt of rings that do not knot or link. In such cases the no-crossing condition sets topological constraints that are inherently nonlocal. The statistical mechanics of such systems is a tremendous theoretical challenge, for which no systematic theoretical tools are presently available. Heuristic approaches [4–10] and ever-growing numerical simulations [11–17] have provided substantial insight, but even basic issues—such as the size of a single ring polymer in a melt or the degree to which different rings mix—are not resolved. Ring polymer melts have received considerable attention as models of chromosome arrangement in the nucleus [18], and experiments on ring melts have revealed unique rheological properties [19]. Additionally, dense systems of open chains may be subject to effective topological constraints on intermediate time scales, yielding very slow relaxation and long-lived "pseudoequilibrium" states with less entanglement than at equilibrium [20,21].

The aim of this Letter is to study the simplest possible (but genuinely many-body) model for a topologically constrained melt. Physically, this model describes directed polymers in quasi-2D, i.e., in a slab geometry, but with the positions of the polymers projected onto the plane to give a 2D lattice model. The remnants of three dimensionality are the fact that the polymers can cross and the crucial distinction between over and undercrossings (Fig. 1). The endpoints of the polymers are held fixed, and the entire melt is constrained to be topologically trivial: that is, continuously deformable to the state in which all polymers are straight lines. The melt is endowed with Monte Carlo dynamics that respect this constraint (i.e., respect the fact that the polymers cannot pass through each other). Mathematically, the polymers form a trivial "braid." The statistical properties of random braids have been studied extensively in order to shed light on polymer topology [22–26], but the dynamical and conformational properties of a topologically constrained melt have not been investigated.

Our model is extremely tractable computationally, so we are able to obtain precise results for its universal properties: these turn out to be surprising in the light of current theoretical ideas. The model is also simple enough to allow hope of analytical progress.

A key feature of the model is that it allows comparison with the predictions of standard theoretical approaches, shedding light on the validity of ideas that are more general

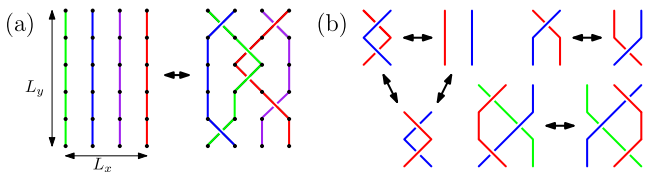

FIG. 1 (color online). (a) Topologically trivial configuration in a small system. (b) Monte Carlo move types. There are six variants of the move on the lower right, and two of that on the upper right.

than the directed case: for example the idea of modeling topological effects in a melt using toy models of a single polymer in an array of obstacles [5,6,10], or the use of Flory-like arguments [7–9]. These approaches are widespread but hard to justify *a priori*. It is important to find ways to confront them with precise results from a genuinely interacting many-polymer model.

The present model may also capture the universal behavior of some realistic situations. The most striking features of our results are expected to extend to systems of directed polymers in 3D, so the results for dynamical behavior may be relevant to relaxation and equilibration in polymer brushes [27,28].

In both the present model and 3D ring melts, topological constraints reduce the extension of individual polymers: entropy dictates that polymers "hide" from each other, as more extended configurations are more likely to be entangled. We will soon see that for directed polymers this effect is almost as strong as it could possibly be.

Model.—Take a number L_x of strands, each of height L_y and directed in the y direction, see Fig. 1(a). At integer y values the polymers lie at integer x values, and all lattice points are occupied. Between y and $y+1$, a given polymer may be vertical, or two neighbors may cross. We take periodic boundary conditions in the x direction, and fix the positions of the endpoints at $y=0$ and $y=L_y$ so the two ends of a given polymer have the same x coordinate. Finally we enforce topological triviality: the allowed configurations are those which can be deformed to the configuration with straight vertical polymers. Mathematically, each configuration C defines an element $g(C)$ of the braid group [29], and allowed configurations are those in which this is the trivial element "1." The partition function Z is the equally weighted sum over allowed configurations (δ is the Kronecker delta):

$$Z = \sum_{\text{configs } C} \delta_{g(C),1}. \tag{1}$$

In practice, to fully define the model we need a Monte Carlo scheme which samples only the topologically trivial configurations. For this we use the moves shown in Fig. 1(b), which have a simple relationship with the defining relations of the braid group [30], and which form a complete set of moves. Intuitively, any local rearrangement can be decomposed into: creation or annihilation of pairs of crossings; motion of crossings; and motion of one strand over or under a crossing between two others. These are precisely the moves in Fig. 1(b). Figure 2 gives an idea of what a subregion of the melt looks like. Note that the model has a fixed monomer density: this eliminates finite-size effects due to fluctuations of the density mode, which is irrelevant to long-distance behavior.

We work in the limit where L_x, the number of strands, is much greater than the typical wandering of the strands.

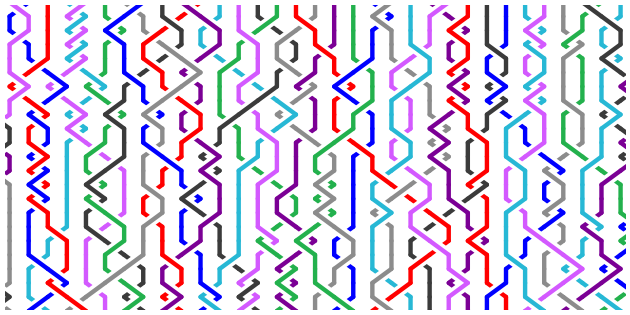

FIG. 2 (color online). A subregion of a topologically trivial melt (taken from a system of size $L_x = 512$, $L_y = 128$).

In fact we enforce a stricter criterion: we ensure L_x is large enough that the results are essentially those of the $L_x \to \infty$ limit. We find that this can be achieved using modest L_x, which is unsurprising given that the wandering is much smaller than L_y. Below we take L_y ranging up to $L_y = 1200$, and L_x ranging up to $L_x = 100$ (larger for some L_y). The Supplemental Material [31] gives further details of simulations, including basic checks of equilibration and convergence in L_x.

Results.—The wandering $D_i(y)$ is defined as the transverse displacement of the ith strand at height y. We denote the root mean square (rms) transverse displacement by $D(y)$. In the *absence* of the topological constraint in Eq. (1), each strand essentially performs a random walk constrained to return to $x_{y=0}$ when $y = L_y$; thus it is clear (and we have checked [31]) that in the unconstrained case $D(L_y/2) \sim \sqrt{L_y}$.

As noted above, the topological constraint will reduce the polymers' wandering. Figure 3 quantifies this using the rms wandering at the midpoint of the strands, $D(L_y/2)$, plotted against L_y. The fit is

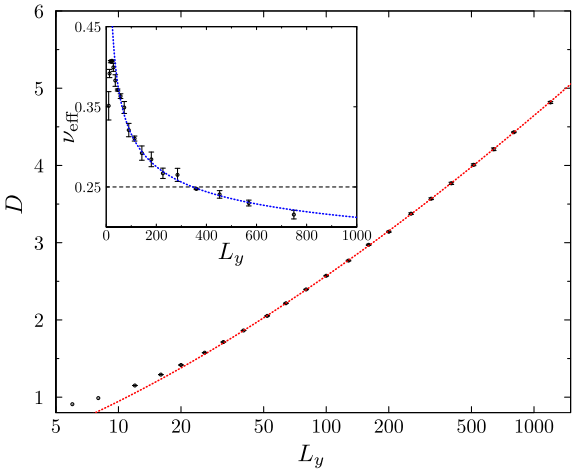

FIG. 3 (color online). Main panel: Transverse wandering D of a strand at its midpoint $y = L_y/2$, as a function of the length L_y of the strands (note lin-log scale). Red line: Fit to the logarithmic form in Eq. (2). Inset: Effective exponent $\nu_{\text{eff}} = d\ln D/d\ln L_y$, see text, with fit derived from Eq. (2).

$$D = A\left(\ln\frac{L_y}{l_0}\right)^{\zeta}, \qquad \zeta = 1.49(3), \tag{2}$$

with $A = 0.26(2)$, $l_0 = 0.91(9)$.

This logarithmic form is unexpected. However, a more conventional power law fit $D \propto L_y^{\nu}$ leads to much worse results, or to an exponent equal to zero within error bars if subleading corrections are included [34]. The inset to Fig. 3 shows an effective finite-size wandering exponent defined by $\nu_{\text{eff}} = d\ln D/d\ln L_y$. This drifts downwards, as expected for the logarithmic form, according to which $\nu_{\text{eff}} \to 0$ as $L_y \to \infty$. The "array-of-obstacles" prediction discussed below, $\nu = 1/4$, is clearly ruled out. See Ref. [31] for further discussion of fits.

Further evidence for the logarithmic behavior comes from the wandering $D(y)$ in the distinct regime $y \ll L_y$. Since no scaling theory exists for this problem, it is not guaranteed *a priori* that the behavior for $y \ll L_y$ and $y \sim L_y/2$ will be similar, but this turns out to be the case. See Fig. 4, where the data fit well to $D(y) = A'(\ln y/l_0')^{\zeta'}$ with $\zeta' = 1.54(15)$. Note the striking agreement between the independently determined exponents ζ and ζ'. The lower inset to Fig. 4 shows the same data on a log-log scale: it is clear from the curvature that a power law would fit only over a very narrow range of scales. The result for $D(y)$ highlights the fact that the properties of a finite-sized subsystem (of height y) are strongly affected by the global topological constraint even in the limit $L_y \to \infty$.

In addition to the rms displacement of a strand, we may consider the full probability distribution. Figure 4 (upper inset) shows this for the displacement at $y = L_y/2$. The data collapses beautifully after rescaling by the rms value. The distribution is not quite Gaussian [31].

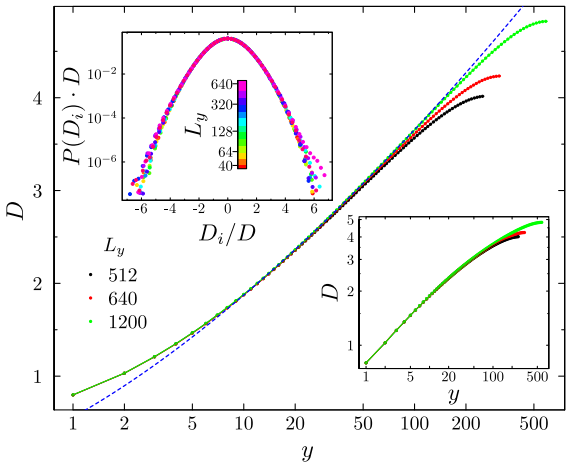

FIG. 4 (color online). Main panel: rms wandering $D(y)$ versus position y along the strand, for various values of the strand length L_y. Blue line: Fit to $D = A'(\ln y/l_0')^{\zeta'}$ for $10 \le y \le 100$, giving $\zeta' = 1.54(15)$, $A' = 0.204(10)$, $l_0' = 0.146(10)$. Lower inset: Same data on log-log plot. Upper inset: Probability distribution for wandering of a strand, $P(D_i)$, rescaled by standard deviation D.

Correlations.—Correlations between the displacements of different strands decay exponentially when their separation is much larger than the wandering. Specifically, let $C_D(x) = \langle D_i D_{i+x}\rangle$, where D_i is the transverse displacement of the ith strand at its midpoint. At large x, $C_D(x) \sim e^{-x/\xi}$, with a correlation length $\xi(L_y)$ that grows in a roughly similar manner to D [31]. The two-point function $C_X(x)$ for the density of crossings (for plaquettes at $y = L_y/2$ separated by a distance x) decays exponentially with period-2 oscillations and a correlation length of less than two lattice spacings.

Dynamics and logarithmic subdiffusion.—The time scale τ for relaxation of the melt is extracted from the Monte Carlo time series. It is independent of L_x for large L_x, but depends nontrivially on the length L_y of the strands:

$$\tau \sim L_y^z, \qquad z = 2.60(6). \tag{3}$$

This exponent describes the equilibration of the entire system within the topologically constrained space of states. The transverse motion of a tagged monomer in an infinite system is more interesting. By Eq. (2), we expect that motion of the monomer by a distance x involves rearrangements of segments of height $y \sim \exp(x/A)^{1/\zeta}$, and a time t which is a power law in y. This implies that the tagged monomer subdiffuses logarithmically slowly:

$$\langle x^2\rangle \sim (\ln t)^{2\zeta}. \tag{4}$$

Similarly, the decorrelation time of a subregion of the melt of size $x \times y$ is exponentially large in x.

Equation (4) describes a monomer inside the topologically trivial melt. It is interesting to ask about the dynamics of a monomer for other choices of the initial state; for example an equilibrated state of the topologically *un*constrained problem. A naive guess might be that the increased local entanglement in such a state will slow the motion even further, but this needs investigation. These issues are related to relaxation in polymer brushes [35], in which the polymers are tethered at one end and are directed (on large scales) for high surface fraction [27,28].

Topological complexity.—The present model allows for a clean definition of the topological complexity of a subregion (the full system is of course topologically trivial). Examining this complexity illuminates the drastic suppression of the wandering. We take the subregion to be the bottom half of the braid, $y < L_y/2$. Fixing the strands' endpoints at $y = 0$ and $y = L_y/2$ gives the half-braid a well-defined topology which cannot be changed by allowed moves in the interior. Allowed moves can, however, reduce the total number of crossings. Let N_{min} be the *minimal* value to which we can reduce this number, and define the complexity per strand as

$$\mathcal{C} = 2N_{\min}/L_x. \tag{5}$$

$\mathcal{C}$ is the average number of crossings encountered (i.e., steps to the right or left taken) by a *single* strand *in the reduced configuration*. $\mathcal{C}$ is finite as $L_x \to \infty$. Note that reducing the half-braid does not change $D_i(L_y/2)$: strands in the reduced half-braid take many fewer steps, but wander by the same total distance.

We compute $\mathcal{C}$ by simulated annealing. Starting with an equilibrated braid, we extract the lower half and subject it to a modified Monte Carlo dynamics with an energy penalty for crossings. The temperature is gradually lowered until the system finds its "ground state." We do not encounter problems finding the ground state [31], perhaps because $\mathcal{C}$ is modest.

The main panel of Fig. 5 shows $\mathcal{C}$ plotted against L_y, and the inset shows the rms wandering $D(L_y/2)$ plotted against $\mathcal{C}$. Strikingly, the wandering has a clean power law dependence on the topological complexity:

$$D \propto \mathcal{C}^{\alpha}, \qquad \alpha = 0.618(2). \tag{6}$$

This implies, for consistency with Eq. (2),

$$\mathcal{C} \propto \left(\ln \frac{L_y}{l_0}\right)^{\eta}, \qquad \eta = \frac{\zeta}{\alpha} \simeq 2.41(6). \tag{7}$$

This is indeed compatible with the results in Fig. 5. For comparison, a braid configuration of height $L_y/2$ chosen uniformly from the set of all such braids has a typical complexity of order L_y [23,24]. For a fixed *finite* number of strands, a sub-braid of sufficiently large height y is believed to have a complexity of order $\sqrt{y}$ [16,22,23], but this is a different ("quasi-1D") limit [31].

The suppression of wandering may therefore be viewed as a consequence of the drastic suppression of complexity.

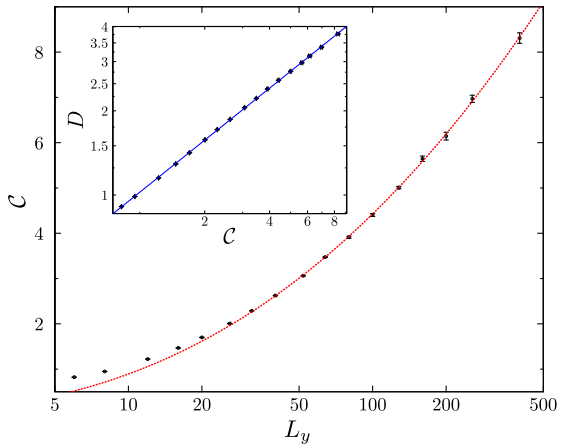

FIG. 5 (color online). Main panel: Complexity (per strand) for the half-braid as a function of L_y, fitted to the form in Eq. (7) with $\eta = 2.6(2)$. Inset: Wandering $D(L_y/2)$ plotted vs the complexity $\mathcal{C}(L_y/2)$ and fitted to a power law, Eq. (6).

Interestingly, the geometry of the strands *in the reduced half-braid* is more conventional than in the unreduced half-braid: the wandering D of a strand has a power law dependence on the average number of steps, $\mathcal{C}$. The exponent α in Eq. (6) is greater than $1/2$, indicating positive correlations between steps in the reduced half-braid. By contrast, the number of steps per strand in the *unreduced* half-braid is much larger, $O(L_y)$, and there are strong negative correlations between steps.

Comparison with standard ideas.—Many approaches to topologically constrained melts rely either on simplifying the problem to a single strand in an array of obstacles which represent the other polymers [4–6,10,36], or on Flory-like free energy arguments [7–9]. These ideas have for example been used to argue that rings in a 3D melt fold up into compact treelike structures [9]. However both approaches are uncontrolled approximations which must be tested against data. For 3D ring melts this is challenging because of large finite-size effects [14,36].

Here, we can make a quantitative comparison with the natural array of obstacles model for the directed case, which describes a single fluctuating strand in an array of straight vertical strands [31]. This predicts $D \sim L_y^{\nu}$ with $\nu = 1/4$, and $\mathcal{C} \sim L_y^{1/2}$ [5], contrary to our results. The wandering distribution also differs [31]. The exponent z on the other hand is roughly compatible with the $z = 5/2$ of the array of obstacles model [10] (though, by the reasoning preceding Eq. (4), the transverse diffusion in the topologically constrained ensemble will be much faster for the array of obstacles). Our results show that, for directed polymers, the behavior of the true melt is very different from the array of obstacles model.

Flory-like estimates are sensitive to the assumed form of the entropic cost of not being entangled [7–9], which is hard to control. Here one can easily show that two-strand interactions alone are not enough to explain $\nu = 0$. See the Supplemental Material [31] for further discussion. The approach does, however, support the expectation that wandering is at least as strongly suppressed in $2+1$D as in $1+1$D.

Throwing out three-strand moves.—Though much simpler than a melt of 3D rings, the present model is still a formidable challenge analytically. One may also consider a reduced model based on the "locally free group" [23,24], a simplification of the braid group. This means imposing the stronger constraint that the melt be deformable to the straight-line state *without* using the three-strand moves of Fig. 1. This is a drastic simplification, and no longer faithful to the topology of directed melts. Nevertheless preliminary simulations suggest that behavior for D remains qualitatively similar, with a reduced $\zeta \sim 1$ [31].

Future directions.—We believe that the crucial features of the present model, including the fact that the wandering is logarithmic (though not necessarily the value of ζ), will carry over to the 3D directed case. This is because the

number of other strands encountered by a given strand grows faster with D in 3D than in 2D, indicating a stronger entropic penalty for wandering. This conjecture must be examined numerically. Another natural next step is to investigate the dynamics of the present model when the endpoints of the chains are free to move, so that the topology of the melt can slowly relax. It would be interesting to know whether the transverse motion of the monomers remains logarithmically slow even in the final equilibrated state. If we start from an unentangled configuration, even the static properties may remain similar to those discussed here for a very long time.

We have seen that for a topologically constrained ensemble of directed polymers, the exponent governing the chains' extension takes its minimal possible value, $\nu = 0$, with logarithmic corrections. One might wonder whether in a 3D ring melt the radius of gyration is also governed by logarithmic corrections to the minimal exponent value ($\nu = 1/3$). Conceivably, such logarithms might partially explain the slow saturation observed for ν in this case.

A fundamental question is whether there exists a real-space renormalization group treatment for topologically constrained polymers [31]. The present model may be simple enough to offer hope of this.

It is a pleasure to thank J. Chalker, J. Haah, M. Kardar, and S. Nechaev for useful discussions and comments. This work was supported in part by Spanish MINECO and FEDER (UE) Grant No. FIS2012-38206 and MECD FPU Grant No. AP2009-0668. P. S. acknowledges the support of EPSRC Grant No. EP/I032487/1. G. B. acknowledges the support of the Pappalardo Fellowship in Physics. A. N. acknowledges the support of a fellowship from the Gordon and Betty Moore Foundation under the EPiQS initiative (Grant No. GBMF4303).

[1] P. G. de Gennes, J. Chem. Phys. **55**, 572 (1971).
[2] P. G. de Gennes, *Scaling Concepts in Polymer Physics* (Cornell University Press, Ithaca, 1979).
[3] M. Doi and S. F. Edwards, *The Theory of Polymer Dynamics* (Clarendon, Oxford, 1986).
[4] S. F. Edwards, Br. Polym. J. **9**, 140 (1977).
[5] A. R. Khokhlov and S. K. Nechaev, Phys. Lett. A **112**, 156 (1985).
[6] M. Rubinstein, Phys. Rev. Lett. **57**, 3023 (1986).
[7] M. E. Cates and J. M. Deutsch, J. Phys. (Paris) **47**, 2121 (1986).
[8] T. Sakaue, Phys. Rev. Lett. **106**, 167802 (2011); Phys. Rev. E **85**, 021806 (2012).
[9] A. Y. Grosberg, Soft Matter **10**, 560 (2014).
[10] S. P. Obukhov, M. Rubinstein, and T. Duke, Phys. Rev. Lett. **73**, 1263 (1994).
[11] M. Müller, J. P. Wittmer, and M. E. Cates, Phys. Rev. E **61**, 4078 (2000).
[12] J. Suzuki, A. Takano, T. Deguchi, and Y. Matsushita, J. Chem. Phys. **131**, 144902 (2009).
[13] T. Vettorel, A. Y. Grosberg, and K. Kremer, Phys. Biol. **6**, 025013 (2009).
[14] J. D. Halverson, G. S. Grest, A. Y. Grosberg, and K. Kremer, Phys. Rev. Lett. **108**, 038301 (2012).
[15] D. Michieletto, D. Marenduzzo, E. Orlandini, G. P. Alexander, and M. S. Turner, ACS Macro Lett. **3**, 255 (2014).
[16] M. V. Imakaev, K. M. Tchourine, S. K. Nechaev, and L. A. Mirny, Soft Matter **11**, 665 (2015).
[17] M. V. Tamm, L. I. Nazarov, A. A. Gavrilov, and A. V. Chertovich, Phys. Rev. Lett. **114**, 178102 (2015).
[18] J. D. Halverson, J. Smrek, K. Kremer, and A. Y. Grosberg, Rep. Prog. Phys. **77**, 022601 (2014).
[19] M. Kapnistos, M. Lang, D. Vlassopoulos, W. Pyckhout-Hintzen, D. Richter, D. Cho, T. Chang, and M. Rubinstein, Nat. Mater. **7**, 997 (2008).
[20] A. Y. Grosberg, S. K. Nechaev, and E. I. Shakhnovich, J. Phys. (Paris) **49**, 2095 (1988).
[21] L. A. Mirny, Chromosome research : an international Journal on the molecular, supramolecular and evolutionary aspects of chromosome biology **19**, 37 (2011).
[22] S. K. Nechaev, *Statistics of Knots and Entangled Random Walks* (World Scientific, Singapore, 1996).
[23] S. K. Nechaev, A. Y. Grosberg, and A. M. Vershik, J. Phys. A **29**, 2411 (1996).
[24] A. M. Vershik, S. Nechaev, and R. Bikbov, Commun. Math. Phys. **212**, 469 (2000).
[25] S. Nechaev and R. Voituriez, J. Phys. A **36**, 43 (2003).
[26] F. Ferrari, Ann. Phys. (Berlin) **11**, 255 (2002).
[27] S. Alexander, J. Phys. (Paris) **38**, 983 (1977).
[28] P. G. De Gennes, Macromolecules **13**, 1069 (1980).
[29] Strictly speaking this differs from the standard braid group by the choice of periodic boundary conditions.
[30] C. Kassel and V. Turaev, *Braid Groups* (Springer-Verlag, New York, 2010).
[31] See Supplemental Material at http://link.aps.org/supplemental/10.1103/PhysRevLett.115.228303 for further details of simulations and toy models. It also includes Refs. [5–7,16,22–24,32,33].
[32] G. S. Grest, K. Kremer, S. T. Milner, and T. A. Witten, Macromolecules **22**, 1904 (1989).
[33] S. Redner and P. J. Reynolds, J. Phys. A **14**, 2679 (1981).
[34] Trying $D = AL_y^{\nu}(1 + BL_y^{-a})$ gives $\nu = 0.10(14)$ and $a = 0.1(4)$.
[35] D. Reith, A. Milchev, P. Virnau, and K. Binder, Macromolecules **45**, 4381 (2012).
[36] A. Rosa and R. Everaers, Phys. Rev. Lett. **112**, 118302 (2014).